Far-Ultraviolet Spectroscopy of the Supersoft X-Ray Binary RX J0513.9−6951

Hutchings, J.B.; Winter, K.; Crampton, D.; Cowley, A.P.; Schmidtke, P.C.

Publisher's version / Version de l'éditeur:
https://doi.org/10.1086/343839
The Astronomical Journal, 124, 5, pp. 2833-2840, 2002

The Astronomical Journal, 124:2833–2840, 2002 November

FAR-ULTRAVIOLET SPECTROSCOPY OF THE SUPERSOFT X-RAY BINARY RX J0513.9−6951[1]

J. B. Hutchings and K. Winter
Herzberg Institute of Astrophysics, National Research Council of Canada, 5071 West Saanich Road, Victoria, BC V9E 2E7, Canada;
john.hutchings@nrc.ca

A. P. Cowley and P. C. Schmidtke
Department of Physics and Astronomy, Arizona State University, Tempe, AZ 85287-1504;
anne.cowley@asu.edu, paul.schmidtke@asu.edu

and

D. Crampton
Herzberg Institute of Astrophysics, National Research Council of Canada, 5071 West Saanich Road,
Victoria, BC V9E 2E7, Canada
Received 2002 June 24; accepted2002 July 29

ABSTRACT

We have obtained spectroscopy with the *Far Ultraviolet Spectroscopic Explorer* of the supersoft X-ray binary RX J0513.9−6951 over a complete binary orbital cycle. The spectra show a hot continuum with extremely broad O VI emission and weak Lyman absorptions. He II emission is weak and narrow, while N III and C III emissions are undetected, although lines from these ions are prominent at optical wavelengths. The broad O VI emission and Lyman absorption show radial velocity curves that are approximately antiphased and have semiamplitudes of $\sim 117 \pm 40$ and 54 ± 10 km s^{-1}, respectively. Narrow emissions from He II and O VI show small velocity variations with phasing different from the broad O VI but consistent with the optical line peaks. We also measure considerable changes in the far-ultraviolet continuum and O VI emission-line flux. We discuss the possible causes of the measured variations and a tentative binary interpretation.

Key words: binaries: close — ISM: jets and outflows — stars: individual (RX J0513.9−6951) — ultraviolet emission — X-rays

1. INTRODUCTION

In this paper we present *Far Ultraviolet Spectroscopic Explorer* (*FUSE*) observations of the supersoft X-ray binary RX J0513.9−6951 (hereafter called X0513−69). This *ROSAT* source was identified with a ∼16th magnitude peculiar emission-line star in the Large Magellanic Cloud (LMC; Pakull et al. 1993; Cowley et al. 1993). With an absolute magnitude of $M_V \sim -2.0$, X0513−69 is the brightest of the supersoft X-ray binaries (e.g., Cowley et al. 1998). It is known to show high and low optical states differing by ∼1 mag (e.g., Alcock et al. 1996; Cowley et al. 2002). The optical spectrum is characterized by strong, broad emission lines of He II and weaker lines of O VI, N V, C IV, and C III. Weak emissions flanking the strongest lines at about ±4000 km s^{-1} have been interpreted as arising in bipolar jets (e.g., Crampton et al. 1996).

Previous spectroscopic work has shown that the emission-line peaks have very small velocity amplitude (e.g., Crampton et al. 1996; Southwell et al. 1996). If these are interpreted as motion of the compact star, the source must be seen at a low orbital inclination and the unseen secondary star must have a low mass. The small amplitude of the optical light curve (Alcock et al. 1996) also suggests the system is viewed from a low inclination angle. However, using a newly refined orbital period and ephemeris, Cowley et al. (2002) have shown that the phasing of the velocities derived from optical spectra differs between the high and low optical states, so that the previously inferred mass function and its interpretation are in doubt.

To access other highly ionized lines (particularly the O VI resonance doublet) and investigate the far-ultraviolet continuum, observations were obtained with *FUSE*. The *FUSE* data presented in this paper add new information about X0513−69.

2. DATA AND MEASUREMENTS

The *FUSE* observations were taken within a 24 hr period on 2001 October 30. The windows during which the system can be observed, between Earth occultations and South Atlantic Anomaly passes, allowed 16 exposures ranging from 367 to 3310 s, spread fairly evenly over ∼1.2 binary cycles. The data were processed using CALFUSE version 2.0.5. The source is bright enough so that there were no difficulties with background subtraction or extraction windows. Analysis of the *FUSE* Fine Error Sensor (FES) images, taken during the acquisition and observation sequence, shows that X0513−69 was in its high optical state at 16.7 ± 0.2 mag during the far-ultraviolet observations.

In general, the LiF1a channel values are the most reliable for wavelength and flux, as this is the guide channel. LiF1b is usually well tracked too, as it suffers little thermal cycling. However, as the observations were continuous, the stability of all the telescope alignments is likely to be good, and the data rates for all channels showed no signs of losing the target star.

Figure 1 shows the mean *FUSE* spectrum of X0513−69, with various features marked. We note the lack of N III or C III lines, although they are present in optical spectra. The principal region of interest is the O VI doublet ($\lambda\lambda$1032, 1038), seen as a broad emission blend, but contaminated by some sharp airglow lines. No broad emissions were seen at

[1] Based on observations made with the NASA-CNES-CSA *Far Ultraviolet Spectroscopic Explorer*. *FUSE* is operated for NASA by Johns Hopkins University under NASA contract NAS 5-3298.

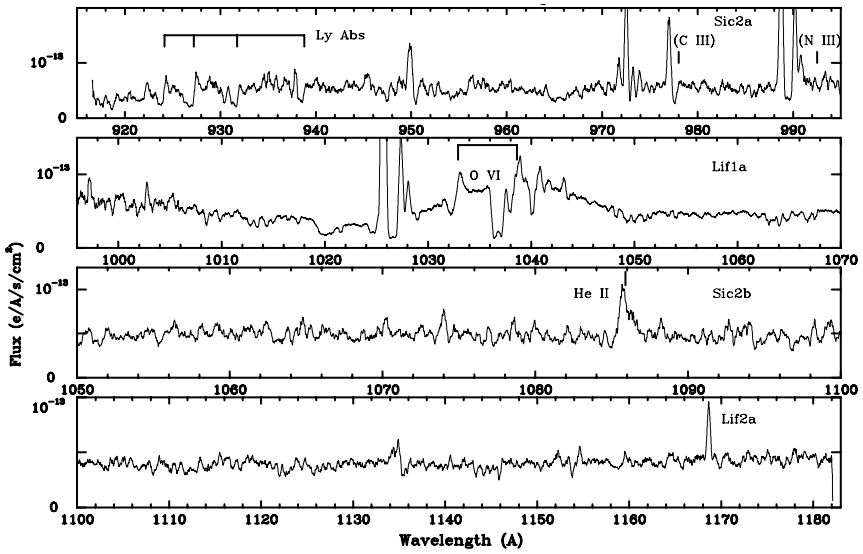

FIG. 1.—Mean *FUSE* spectrum of X0513−69. Each panel is from one *FUSE* spectral channel, as identified, so the wavelength scales differ and overlap somewhat. Emission features are airglow lines, except for He II and O VI, as marked. Some of the Lyman absorption lines that arise in the binary system are identified, and the positions of the nondetected C III and N III lines are shown. All identifications are shifted to the LMC velocity frame.

other less ionized lines, such as He II, C III, or N III. There are also weak sharp emissions at the positions of the O VI lines, unfortunately blended with airglow and interstellar absorption features. However, the relative strengths of these and other unblended airglow lines indicate that the sharp O VI peaks are present, superposed on the broad emission. We note that the weak O VI lines in the visible region (Crampton et al. 1996) are seen only as sharp peaks, with no broad component detected. In the *FUSE* spectra He II is detected only as a sharp emission peak, weak and blended with airglow emissions. By contrast, both a strong narrow component and broad emission wings are seen in the He II line at 4686 Å. In *Hubble Space Telescope* spectra, Gänsicke et al. (1998) found a similarly broad structure in the N V resonance doublet ($\lambda\lambda$1239, 1243), also with narrow peaks (see their Figs. 1 and 4). The continuum is present throughout the entire *FUSE* range, and there are narrow Lyman absorptions, seen most clearly in lines Lyδ through Lyζ.

Table 1 gives the observational details and some of the measurements made. In all cases, the new ephemeris by Cowley et al. (2002) is used. The eight different *FUSE* spectral channels were measured separately. Those with the best

TABLE 1
MEASUREMENTS OF *FUSE* DATA FOR RX J0513.9−6951

Spectrum	HJD Mid-Exposure (2,452,210+)	Phase[a]	Exp. Time (s)	Broad O VI Emission RV[b] (km s^{-1})	Broad O VI Emission Flux[c]	Lyman Abs. RV[d] (km s^{-1})	1040 Å Continuum[e]
1.....	3.431	0.87	1571	1201	7.6	200	3.6
2.....	3.502	0.97	1239	1227	8.4	280	4.1
3.....	3.570	0.06	973	916	8.3	283	4.2
4.....	3.611	0.11	367	930	10.5	290	6.4
5.....	3.643	0.16	918	963	9.3	350	4.3
6.....	3.684	0.21	801	965	7.0	313	5.2
7.....	3.714	0.25	650	740	8.8	291	4.9
8.....	3.755	0.30	1230	934	6.5	240	4.4
9.....	3.827	0.40	1610	1147	6.2	214	4.0
10.....	3.906	0.50	3240	1153	4.9	185	3.1
11.....	3.976	0.59	3310	1217	4.8	197	3.0
12.....	4.045	0.68	3298	1156	5.3	196	3.0
13.....	4.114	0.77	3281	1026	5.1	186	3.1
14.....	4.184	0.86	3281	1190	4.9	184	3.2
15.....	4.257	0.96	2571	1099	5.6	229	3.3
16.....	4.328	0.05	1832	1159	6.4	166	3.4

[a] Ephemeris: T_0 = JD 2,448,858.099 + 0.7629434E days, where T_0 is the time of V_{MACHO} minimum light (see Cowley et al. 2002).
[b] Uncertainties are ±40 km s^{-1}.
[c] Units of 10^{-13} ergs s^{-1} cm^{-2}.
[d] Uncertainties are ±20 km s^{-1}.
[e] Mean value, units of 10^{-14} ergs s^{-1} cm^{-2}.

signal level are reported here. Measurements of the *FUSE* spectra were made by fitting single profiles to the O VI emission blend and also by cross-correlation against a smoothed mean spectrum template, which had been edited to remove airglow emission and narrow interstellar absorptions. Airglow emissions were identified using the atlas in Feldman et al. (2001) and also by comparing spectra with varying fractions of nighttime in the exposure. The Lyman absorption lines were measured by simple profile fitting. The continuum variations were measured by averaging the total fluxes outside the emission features with airglow emissions removed. Figure 2 shows plots of the measured quantities, and Figure 3 shows the O VI profile in detail and a montage of changes with orbital phase. We discuss the broad O VI in detail in the following section.

Since there was a large range in individual exposure times among the spectra listed in Table 1, we generated a set of nine spectra combined to equalize their exposures and phase coverage and hence enhance the signal-to-noise ratio for measurement of the weaker features. These were also used as a check for our major results. In all cases these phase-averaged spectra gave similar results, so we do not quote these measures in detail. We note, however, that there are differences in some measures between the overlapping phases from the two orbital cycles covered. Further observations would be required to fully separate the phase-dependent and irregular changes.

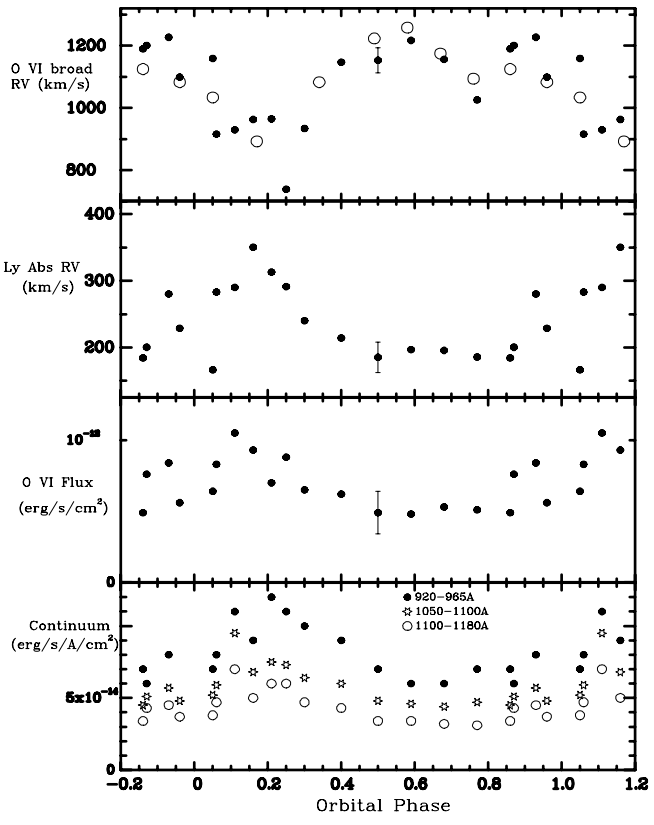

FIG. 2.—Measured quantities in X0513−69 plotted against orbital phase. Typical error bars are shown for the velocity measurements. The O VI velocities are the average of cross-correlation and profile-fitting measures and are shown for all spectra (*filled circles*) and for spectra binned for equal signal (*open circles*). The continuum values in the bottom panel are fitted continuum levels and not the total signal as in Table 1. Although the variations are not sinusoidal, O VI emissions and Lyman absorptions appear to vary in antiphase. The orbital phases are based on the new Cowley et al. (2002) ephemeris.

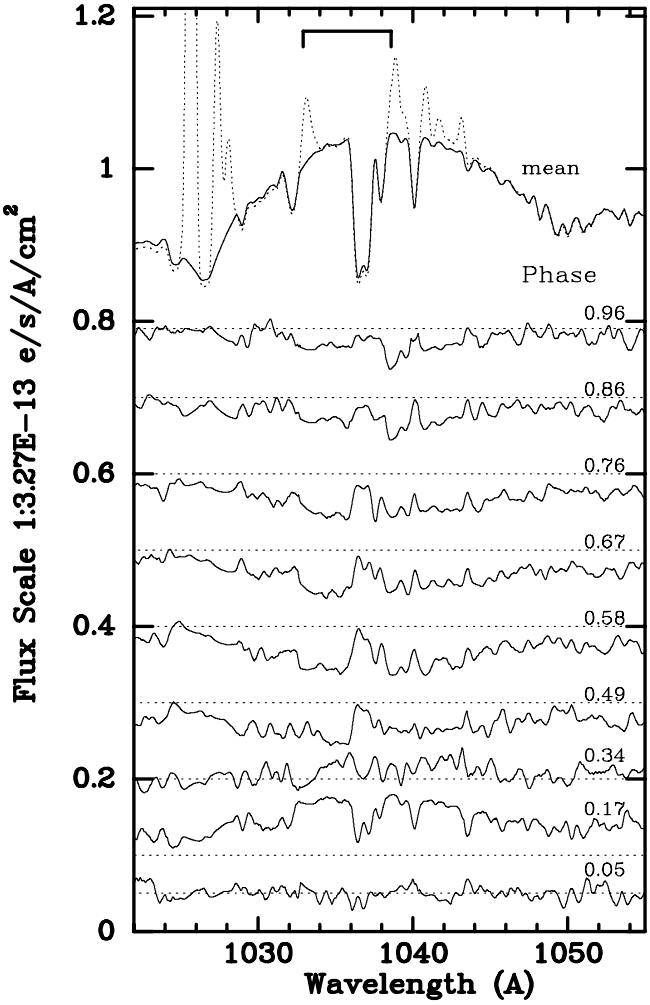

FIG. 3.—Mean O VI doublet profile with airglow and peak emission shown as edited out (*top*). The position of the O VI lines with an LMC velocity are marked. The airglow emissions are sharper than shown here in the heavily smoothed plot, so that the contamination by airglow is less severe than the plot suggests. The absorption lines are interstellar. Below the mean spectrum are individual spectrum differences from the mean, edited of airglow, plotted by phase. These are derived from the set of nine phase-binned spectra. Overall changes are seen to be smooth and symmetric across the profile center, indicating that there are no broad profile shape changes.

All measurements were run through a sine-wave–fitting program to determine relative binary phases of their variations, using the Cowley et al. (2002) ephemeris. The results and their formal errors are shown in Table 2. Inspection of Figure 2 shows that some variations are not very sinusoidal, especially the velocity curves of the broad O VI emission and Lyman absorption, but the formal errors of the fits are a useful measure. Using more complex functions, such as elliptical orbit fits, does not alter the amplitudes and phasing significantly. Note that the phase errors are all quite small, with the exception of He II emission velocities.

3. O VI BROAD EMISSION

The O VI emission is extraordinarily broad and cannot be separated into the two O VI lines at 1032 and 1038 Å. Moreover, the whole emission feature is redshifted by some

TABLE 2
PHASING OF FUV SPECTROSCOPIC VARIATIONS IN RX J0513.9−6951

Data	HJD (Time of Max.)	Semiamplitude K	Mean Error	Binary Phase[a]	Sine-Fit Mean
Radial velocity (km s^{-1}):					
O VI mean emission[b]	2,452,214.00 ± 0.05	126 ± 55	152	0.62 ± 0.07	1141 ± 41
O VI cross-corr. emission	2,452,214.07 ± 0.04	110 ± 36	94	0.71 ± 0.06	1094 ± 26
Binned spectrum, mean	2,452,214.06 ± 0.03	121 ± 30	64	0.70 ± 0.05	1118 ± 22
Adopted	...	117	...	0.70	...
H Lyman absorption	2,452,213.64 ± 0.02	54 ± 10	23	0.15 ± 0.02	226 ± 7
He II emission	2,452,213.56 ± 0.19	11 ± 11	22	0.05 ± 0.25	268 ± 7
Line flux (×10^{-13}):[c]					
O VI	2,452,213.63 ± 0.02	2.0 ± 0.4	1.2	0.14 ± 0.03	6.4 ± 0.3
He II	2,452,214.00 ± 0.06	0.27 ± 0.15	0.30	0.62 ± 0.08	0.46 ± 0.01
O VI equivalent width (Å):					
Mean[b]	2,452,213.51 ± 0.05	2.3 ± 0.9	3.0	0.15 ± 0.06	17 ± 1
Continuum (×10^{-14}):[c]					
920–965 Å	2,452,213.71 ± 0.04	2.0 ± 0.4	1.1	0.24 ± 0.03	7.0 ± 0.3
1050–1100 Å	2,452,213.69 ± 0.03	1.5 ± 0.3	0.9	0.22 ± 0.03	5.6 ± 0.2
1100–1180 Å	2,452,213.68 ± 0.02	1.3 ± 0.3	0.7	0.20 ± 0.03	4.2 ± 0.2
Optical He II peaks (km s^{-1}):					
High optical state	2,449,669.93 ± 0.02	11.2 ± 2.2	7.5	0.08 ± 0.03	279 ± 2
Intermediate optical state	2,449,669.78 ± 0.03	11.8 ± 2.4	8.9	0.88 ± 0.04	299 ± 2

[a] Ephemeris: T_0 = JD 2,448,858.099 + 0.7629434E days, where T_0 is the time of $V_{\rm MACHO}$ minimum light (see Cowley et al. 2002).
[b] Mean of profile fits to LiF1A, LiF2B, and SiC2A.
[c] Flux units are ergs s^{-1} Å^{-1} cm^{-2}.

800 km s^{-1} or more (∼3 Å) from the mean wavelength expected for the blend at the velocity of the LMC. The profile is complicated by the presence of strong C II λ1036 and other weaker interstellar absorptions and by airglow emissions, including the strong Lyβ line at 1026 Å. Figure 3 shows the mean O VI profile and its variation with phase.

It appears that the emission actually extends to about ±4000 km s^{-1}, but there is a P Cygni absorption that erodes the short-wavelength side. The amount of O VI absorption is evident from the difference between the profile and its reflection about zero velocity, which is shown in Figure 4. Zero velocity is taken as the mean wavelength of the two O VI lines, shifted by the systemic velocity (about +280 km s^{-1}). This assumes equal flux from each line (i.e., high optical depth). This means that the velocity width for each individual line is ∼3000 km s^{-1}.

The high-velocity optical jets seen in H and He II lines (Crampton et al. 1996; Southwell et al. 1996) do not appear to have a counterpart in the far-ultraviolet O VI lines. In the optical region, the jet lines stand well above the broad wings in most observations, while Figure 4 shows a smooth profile with no features at ±4000 km s^{-1}. However, we note that the optical jet lines are variable from epoch to epoch. Cowley et al. (1998) found the jet lines very weak or absent in spectra taken in 1996 during a bright optical state, whereas they had been detected easily in 1993 and 1994 spectra (see their Fig. 3). The broad O VI emission profiles do extend out to these high velocities, as do the He II λ4686 wings, but the λ4686 wings could not be measured accurately for radial velocity changes because of blending with the nearby N III/C III blend. However, Crampton et al. did report extended shortward absorption in the broad wings of Hβ, indicating a similar P Cygni wind profile as seen in O VI (see Fig. 4).

There are at least three possible causes of the measured broad emission radial velocity variations. These include (1) changing strength of the P Cygni absorption, altering the mean position of the unabsorbed emission, (2) variation of the relative strengths of the two O VI doublet lines, corresponding to changes in the optical depth of the emission region, and (3) velocity variations that reveal orbital motion of the emission-line region.

Both possibilities 1 and 2 above would involve changes in the overall profile of the emission feature. Crampton et al. (1996) report that in their 1994 data "the Hβ wind absorption appears to be strongest at phase 0.75" (which is phase 0.72, using the revised ephemeris of Cowley et al. 2002), but from limited data they also note that the "changes are of low significance and may not be phase related." This phas-

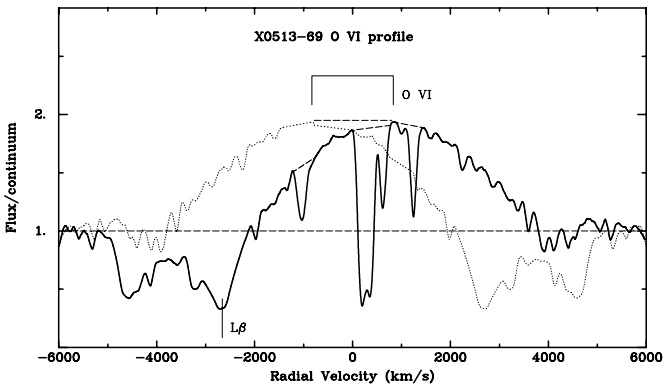

FIG. 4.—Mean O VI profile folded in velocity space about the mean LMC wavelength of the doublet. There appears to be a strong P Cygni absorption underneath a broad emission that reaches to some 4000 km s^{-1}, causing the large apparent wavelength shift of the emission. There are weak peaks from each of the O VI lines that are blended with airglow emission and interstellar absorptions.

ing corresponds roughly to the maximum velocity of the broad O VI emission, suggesting the velocity variation might be related to changing P Cygni absorption strength. However, in the *FUSE* broad O VI profiles we do not see such a change, but rather only changes in the overall emission flux (plus associated changes in the interstellar absorption depths). Profile changes that give rise to the measured full velocity amplitude of $\sim$240 km s^{-1} would show up as a profile difference, significantly different on the opposite sides of the central wavelength. This is not seen at any phase, particularly not between the phases of maximum velocity differences, where we see the expected "sine wave" difference spectrum from a moving but unchanging profile. We thus consider that the broad profile arises in a region that appears similar from all viewing angles.

The phasing of the measured velocity curve is close to that expected for the compact star's orbital motion, assuming the optical light minimum occurs near its superior conjunction (Cowley et al. 2002). Thus, we consider the implications of possibility 3. The small velocity amplitude of the peak emission velocities was discussed in this context by Crampton et al. (1996) and Southwell et al. (1996). Their interpretation implies either a low orbital inclination or a low-mass donor star ($\sim$0.3 $M_{\odot}$). However, as shown by Cowley et al. (2002), the new ephemeris makes this model unlikely, since maximum velocity does not occur at the expected phase. Therefore, we explore the possibility that the $\sim$120 km s^{-1} semiamplitude of the O VI broad emission is an upper limit to the compact star's motion. If there are small profile changes that contribute to the velocity amplitude, they will reduce the contribution from the orbital motion. Thus, this measured velocity gives a maximum value to the mass function for the system. We discuss the implications in more detail below.

The very broad O VI emission most likely arises in the innermost parts of the accretion disk, as this is where we expect the most highly ionized material to be found if radiatively excited. We argue below that the mass of the compact star probably lies in the range 0.7 to 1.1 $M_{\odot}$, while the orbital inclination must be $\sim$35°, given the line widths. The orbital velocity at the surface of such a white dwarf is in the range 3100 to 5500 km s^{-1}, which would be projected to 1900 to 3400 km s^{-1} for an equatorial disk that reaches the stellar surface. The emission profile from such a disk at this inclination angle would not be strongly double-peaked, and the blend of two O VI line profiles (separated by some 1700 km s^{-1}), together with interstellar absorptions, would further obscure any profile structures.

An alternative site for high velocities in the O VI profile is the bipolar jets. As noted, the jets are seen in much lower ionization lines as two separate and relatively narrow peaks, implying a high degree of collimation. The O VI could conceivably arise in the inner accelerating part of the jets. However, since the jets are highly collimated (the jet emissions indicate an opening angle less than 10°), this would give rise to very double-peaked structure at any point in the jet, quite unlike the profiles seen in the *FUSE* data.

Given the probable origin of the broad emission in the inner disk and its unchanging profile with phase, we note that the P Cygni absorption must indicate a considerable (and azimuthally symmetric) disk wind that is seen around the viewing cone and which must be separate from the jets. Absorption within a jet would be seen only in a narrow viewing cone of about half the 10° jet opening angle.

4. FUV LIGHT CURVE AND OTHER LINE FEATURES

The continuum is detected throughout the *FUSE* spectral range. Continuum variations were measured by averaging the total fluxes in regions outside the emission features where the airglow emissions had been removed. The measured flux changes are shown in Figure 2 and in Tables 1 and 2. Table 1 shows values of the interpolated continuum at the O VI doublet, while the values in Table 2 and Figure 2 are continuum levels fitted uniformly to the wavelength regions indicated. The agreement between the independent *FUSE* channels is very good. Note the rising flux level to shorter wavelengths, indicating very high temperatures. Expressed in magnitudes, the orbital variation is $\sim$0.5–0.6 mag, but examination of overlapping phases shows this amplitude is partially due to cycle-to-cycle variations. The far-ultraviolet (FUV) variation is much larger than that seen in the optical, where the mean range is only $\sim$0.04 mag, but the cycle-to-cycle variations are up to $\pm$0.2 mag (see Cowley et al. 2002).

To be so much larger in the FUV, the FUV continuum and its changes must come from a region with temperatures of 30,000 K or more. We also note that the O VI broad emission flux varies with similar amplitude and phasing, so it is likely to be associated with the continuum changes. Since disk light dominates the spectrum, we are seeing azimuthally varying disk brightness. One possibility is a thickening of the outer disk downstream of the gas stream from the donor star. Illuminated by the hot inner disk, this would be brightest when viewed from the opposite side. We discuss below a model in which the phasing of this is consistent with the radial velocity changes.

Cowley et al. (2002) discuss the origin of the optical light variations, showing the phasing of the minima has persisted for at least 8 years. Thus, it is likely to be caused by a geometric occultation of a bright region fixed within the system, rather than disk structure whose position and shape may change. This region may be the inner point in the Roche lobe, where heating by the white dwarf (WD) and X-rays is greatest. Thus, they suggest that phase 0 is at or close to superior conjunction of the compact star. We adopt this geometry in our binary discussion below.

It was not possible to make clean measures of the O VI peak emissions, because of blending with the airglow and interstellar lines. The 1038 Å line velocity shows a correlation with the fraction of the exposure that was in daylight (i.e., strength of airglow). If we fit a straight line through this, we find a velocity of +295 km s^{-1} for an airglow-free spectrum, which is close to the systemic velocity. If we examine the deviations from this line as function of binary phase, there is a small amplitude variation ($K \sim 10$ km s^{-1}), with maximum close to phase 0, as was found by Cowley et al. (2002) for He II peaks during the bright state. Since our examination of the FES image indicates X0513−69 was in a high optical state during the *FUSE* observations, it appears that the narrow O VI λ1038 component probably behaves like the He II λ4686 peaks.

The 1032 Å line is more strongly blended by the interstellar absorption on its shortward side, and the measures of this line give a scatter about apparent velocity +380 km s^{-1}. Both line peaks show apparent flux changes, which are also attributable to blending with airglow lines and the small velocity variations noted above for the 1038 Å line.

The narrow He II emission at 1084 Å is weak and has airglow lines nearby. However, we do measure a low velocity amplitude (similar to the He II 4686 Å optical line of Crampton et al. 1996) and a phasing that is different from the broad O VI, but close to that of the O VI λ1038 peak mentioned above.

Table 2 includes our fits to the optical emission peak velocities from Crampton et al. (1996) and Southwell et al. (1996) for the optically bright and the transition states, using the new ephemeris. We note that the *FUSE* He II peak velocities, while poorly determined, are quite consistent with the high-state optical velocity phasing and amplitude. This is also included in our binary orbit discussion below. The He II peak flux shows a small change that is maximum at phase 0.62 (see Table 2), if the changes are phase-related.

Lyman absorptions are clearly present at all phases, and they are seen well down the series. The stronger Lyman lines have severe airglow contamination, but the airglow has a strong decrement, and the lines measured are free of any significant airglow contamination, as determined by extrapolation of the decrement. There is a weak correlation of radial velocity with fraction of nighttime in the exposure (hence potential strength of airglow), but less than half the amplitude with orbital phase, and there is no measurable change in the equivalent width with phase or with nighttime fraction. The absorption mean velocity is +226 km s^{-1}, suggesting an outflow from X0513−69 whose systemic velocity is about +280 km s^{-1} (and not consistent with contamination by zero-velocity airglow). We note that the Lyman absorption velocity changes are closely phased with the increase in broad O VI flux. If a broad Lyman emission within the system increases during the same phases, then it could conceivably produce a line asymmetry, causing the Lyman absorption to be measured more positively. However, the Lyman absorptions are only 1 Å wide, compared with 18 Å for the broad emission. We discuss below the puzzle of where the neutral absorber may be that gives rise to these absorptions, but we draw attention (see Table 2) to the fact that the velocity changes are close to being antiphased with the broad O VI emission velocity.

5. A POSSIBLE BINARY MODEL

Here we examine the implications of assuming that the broad O VI emission velocity curve reflects the orbital motion of the compact star in X0513−69. Adopting the amplitude and phasing given in Table 2, we have adopted a weighted mean of the profile-fitting and cross-correlation measurements, using both the individual spectra and also the phase-binned spectra of equal signal. The sketch in Figure 5 shows how the measured quantities vary with binary phase. Following Cowley et al. (2002), we assume phase 0 occurs at the superior conjunction of the compact star, and the phasing of the FUV measures are based on this new ephemeris. The broad O VI emission velocity phases are consistent with them showing the orbital motion of the WD, within their uncertainties (Table 2). The high-state light curve of Cowley et al. has a wide minimum, centered at phase 0 as derived from a sine-curve fit to the individual data points. In the fainter, "transition" state the minimum may be narrower, but it is also centered on phase 0. We stress that there is an uncertainty about what is causing the optical minimum, so that assuming it occurs at conjunction

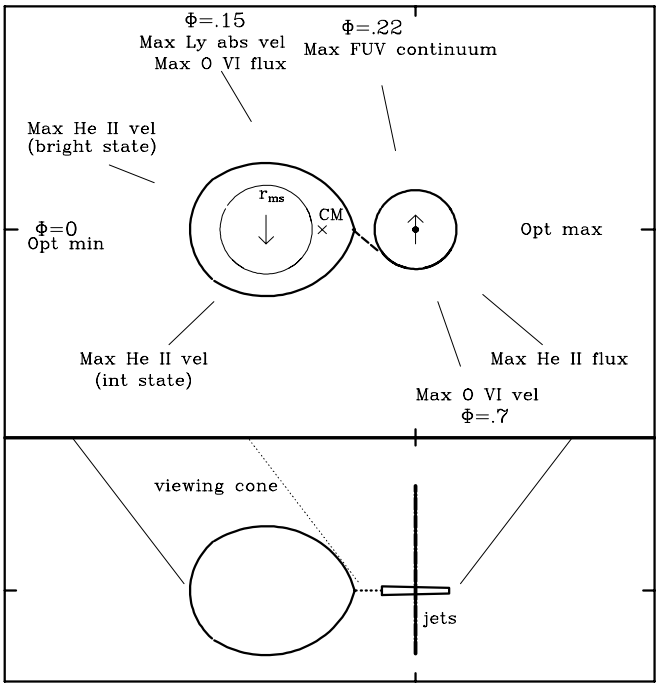

FIG. 5.—Sketch of the binary system as proposed, with the key measured quantity variations indicated. The text discusses where the various spectral features appear to arise. The circle inside the donor star shows the main-sequence radius of a star of the mass discussed. The bottom panel suggests the viewing cone, if the orbital inclination angle is $i = 35°$.

may be incorrect. There might instead be an off-centered brighter region that is partially hidden at phase 0, but it is unlikely to be a structure in the disk, since it was stable for over 8 years.

The lack of significant profile changes suggests that the major source of broad O VI is in the inner parts of the accretion disk, rather than in a stream or the inner part of the Roche lobe where narrow components might be formed. By contrast, we note that the O VI emission seen in AM Her, a highly magnetic catalysmic variable without a disk, has a complex and varying profile, and the lines do appear to arise in other parts of the system where shock heating may ionize the O VI (Hutchings et al. 2002).

For X0513−69, the adopted semiamplitude of 117 km s^{-1} for the compact star gives a mass function that implies the values shown in Figure 6. The lack of any eclipse in the light curve at any wavelength indicates that the orbital inclination is less than $\sim 60°$. The considerable width of the broad emission argues against a very low orbital inclination angle. On the other hand, the observed high velocity of the bipolar jets, which presumably are oriented nearly perpendicular to the disk, is expected to be close to the escape velocity for the white dwarf (e.g., Southwell et al. 1996). At a higher orbital inclination, their observed velocities would be expected to be much lower (as seen in the supersoft binary RX J0019.8+2156; Cowley et al. 1998).

These considerations are shown in Figure 6. The dashed lines show the locus where the projected jet velocity equals the escape velocity for the white dwarf and also the locus of the projected orbital velocity at its equator. The jet velocity is assumed not to exceed escape velocity, and the line width not to exceed orbital velocity at the white dwarf surface. The diagram shows a region where both conditions apply.

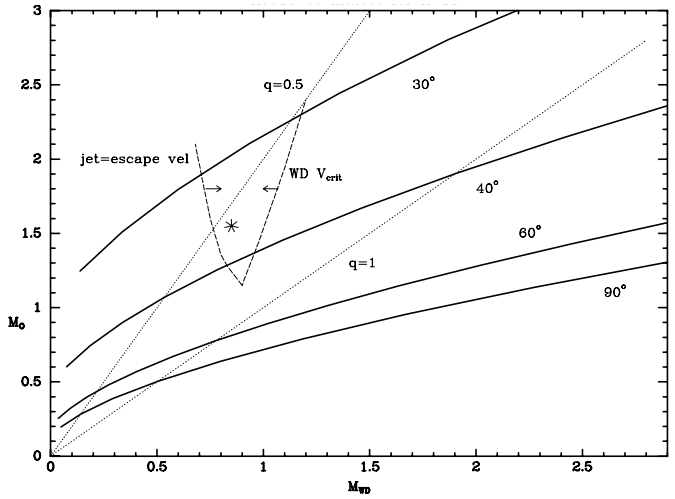

FIG. 6.—Mass diagram for the binary system for various orbital inclinations, from the broad O VI velocities. The likely range of values is indicated by the dashed lines, which are the limits defined by the jet velocity and broad line width. The asterisk represents the value discussed in detail in the text.

We consider white dwarf masses between 0.7 and 1.1 $M_\odot$ and inclinations above $\sim 30^\circ$ to be feasible. We discuss below a mass ratio of ~ 2 and a donor star mass of $\sim 1.6\ M_\odot$, with an orbital inclination of 35°. Figure 5 shows a sketch of the Roche lobe and center of mass for this mass ratio.

The WD orbital velocity, with an inclination angle $\sim 35^\circ$, sets the donor star Roche radius (polar) at $\sim 1.7\ R_\odot$. The main-sequence radius of a star of mass $1.6\ M_\odot$ is $\sim 1.2\ R_\odot$. This is also sketched in Figure 5, and it lies well within the Roche lobe. On the other hand, a giant (luminosity class III) of this mass will have a radius of $\sim 4.5\ R_\odot$, which would engulf the companion. Thus, we suggest that the donor star is just at the end of its main-sequence lifetime and expanding. This would imply a large mass transfer rate and bright disk, as observed. X0513−69 is several times brighter visually than other supersoft X-ray sources (SSSs) in the LMC (e.g., CAL 83 and CAL 87), although its bolometric luminosity is similar to that of CAL 83 ($L_{\rm bol} \sim 5 \times 10^{38}$ ergs s^{-1}). Both CAL 83 and X0513−69 also show bipolar jets, which are characteristic of a luminous disk. The absolute magnitude of a $1.5\ M_\odot$ main-sequence star is about +3 (+1.3 for a giant), while the whole X0513−69 system has absolute magnitude of −2.0. Thus, the lack of visibility of the proposed donor star is not surprising, as it is only a few percent of the disk luminosity. Indeed, if the optical light curve is due to heating of the donor star, as in the case of HZ Her, the observed amplitude is about that expected for any noneclipsing inclination.

In this model, disk thickening by gas-stream impact is seen from the far (illuminated) side of the disk at the phase shown for maximum FUV light. The He II and O VI peak velocity probably arises in or near the intersection of the mass stream and disk, as seen in other X-ray binary systems (e.g., Cyg X-1). This material lies near the system center of mass and has a low velocity vector, which is the sum of the stream and orbital velocity at this point. In the low optical state, when the disk is fainter (smaller?), the relative change of orbital and streaming velocity vectors leads to the observed change in phase of maximum peak velocity, as sketched. The optical minimum may be caused by the partial occultation of the inner point of the Roche lobe where the donor star will be brightest. The He II λ1085 peak flux is maximum at phase 0.62, which is where the heated donor star is most clearly visible. However, the feature is weak and near variable airglow lines.

The Lyman sharp absorption velocities are antiphased with the broad O VI, and thus they suggest association with the donor star. However, the disk and not the donor star must be the source of the FUV continuum radiation behind the absorbing material. Also, as mentioned earlier, the absorption lines have a mean velocity of +226 km s^{-1} compared with the systemic velocity of +280 km s^{-1} obtained from the optical He II emission lines. Thus, we may be looking through a ~ 50 km s^{-1} outward flow of cool material that arises from the donor star and is projected against the hot continuum of the disk. The absorbing column does not vary measurably with binary phase, but the lines are weak and the continuum does vary. However the absorptions arise, they may still carry the orbital motion of the secondary. It is hard to imagine another way they could be antiphased with the broad O VI emission. It is interesting that this yields a mass ratio for the stars of $54/117 = 0.46$, which lies right in the region we have already noted in Figure 6. However, the Lyman absorption velocity curve is far from sinusoidal, so perhaps the origin of these lines lies elsewhere.

The masses suggested here are unusual for SSSs in having a more massive donor star. As noted, it is possible that the real mass function is lower, if some of the measured broad velocity changes are due to profile changes. However, we have suggested that such a contribution would be small, so we regard the mass discussion as an upper limit of interest. The disk in this system is extremely luminous, and it is widely assumed that the disk brightness and jet formation occur because the mass transfer rate is high. Thus, this is consistent with a more massive donor star. As pointed out by Cowley et al. (2002), the binary model implied by the much lower velocity amplitude of the optical line peaks (Crampton et al. 1996; Southwell et al. 1996) is no longer consistent with the revised ephemeris from the optical light curve. Other problems with this original model were the very low inclination (nearly pole-on) and the low donor star mass, if one assumed the compact star was a white dwarf.

It was originally suggested by van den Heuvel et al. (1992) that the donor stars in supersoft binary systems would be expected to be about twice the mass of the white dwarf, based on evolutionary considerations. However, until the present data on the FUV O VI velocities, all previous observational evidence has indicated the donors are low-mass stars (see, for example, review by Gänsicke et al. 2000). As this system appears to differ from other SSSs in having a more massive donor star, it may be that the mass transfer can be driven by more than one mechanism. In this case, normal Roche lobe overflow by evolution off the main sequence would apply, while for the less massive donor stars, an additional wind mechanism is required.

We are grateful to Alex Fullerton for processing the observations independently of the regular data pipeline. A. P. C. acknowledges her support from NASA and the National Science Foundation.

REFERENCES

Alcock, C., et al. 1996, MNRAS, 280, L49
Cowley, A. P., Schmidtke, P. C., Crampton, D., & Hutchings, J. B. 1998, ApJ, 504, 854
Cowley, A. P., Schmidtke, P. C., Hutchings, J. B., & Crampton, D. 2002, AJ, 124, 2233
Cowley, A. P., Schmidtke, P. C., Hutchings, J. B., Crampton, D., & McGrath, T. K. 1993, ApJ, 418, L63
Crampton, D., Hutchings, J. B., Cowley, A. P., Schmidtke, P. C., McGrath, T. K., O'Donoghue, D., & Harrop-Allin, M. K. 1996, ApJ, 456, 320
Feldman, P. D., Sahnow, D. J., Kruk, J. W., Murphy, E. M., & Moos, H. W. 2001, J. Geophys. Res., 106, 8119
Gänsicke, B. T., van Teeseling, A., Beuermann, K., & de Martino, D. 1998, A&A, 333, 163
Gänsicke, B. T., van Teeseling, A., Beuermann, K., & Reinsch, K. 2000, NewA Rev., 44, 143
Hutchings, J. B., Fullerton, A. W., Cowley, A. P., & Schmidtke, P. C. 2002, AJ, 123, 2841
Pakull, M. W., Motch, C., Bianchi, L., Thomas, H.-C., Guibert, J., Beaulieu, J. P., Grison, J. P., & Schaeidt, S. 1993, A&A, 278, L39
Southwell, K. A., Livio, M., Charles, P. A., O'Donoghue, D., & Sutherland, W. J. 1996, ApJ, 470, 1065
van den Heuvel, E. P. J., Bhattacharya, D., Nomoto, K., & Rappaport, S. A. 1992, A&A, 262, 97